

Infrared, Raman spectroscopy and ac magnetic susceptibility of Gd_2O_3 - TeO_2 - V_2O_5 glasses

Y. B. SADDEEK, I. S. YAHIA^{a*}, W. DOBROWOLSKI^b, L. KILANSKI^b, N. ROMČEVIĆ^c, M. ARCISZEWSKA^b

Department of Physics, Faculty of Science, Al-Azhar University, Assiut, Egypt

^aDepartment of Physics, Faculty of Education, Ain Shams University, Roxy, Cairo, Egypt

^bInstitute of Physics, Polish Academy of Sciences, Al. Lotnikow, 32/46, 02-668 Warszawa, Poland

^cInstitute of Physics, Pregrevica 118, 11080 Belgrade, Serbia

In this paper, we present a characterization of the local structure and magnetic properties of the glassy system xGd_2O_3 -65 TeO_2 -(35-x) V_2O_5 (x = 2.5, 5, 7.5 mol %) using IR and Raman on one hand, and ac magnetic susceptibility measurements on the other hand. Analysis of IR and Raman spectroscopy indicates to the presence of four main bands attributed to the structural units $[TeO_3]$, $[TeO_4]$, $[VO_4]$, and $[VO_5]$, respectively. The presence of gadolinium cations in the glass structure leads to the appearance of a structural ordering process around the vanadium atoms as well as to a decrease in the number of linked tellurium polyhedra. Thus, it can be said that Gd^{+3} may significantly modify the Te-O network. The ac magnetic susceptibility, the magnetic moment and the Curie temperature, the molecular field constant of these materials were investigated in a temperature range of 4–200K. The reciprocal of the molar magnetic susceptibilities of all samples appear to obey Curie-Weiss law in the paramagnetic region.

(Received May 15, 2009; accepted June 15, 2009)

Keywords: Tellurite glasses, IR and Raman spectroscopy, Ac magnetic susceptibility

1. Introduction

Tellurium oxide (TeO_2) based glasses are of scientific and technological interest on account of their unique properties such as chemical durability, electrical conductivity, transmission capability, high dielectric constant, high refractive indices, good infrared transmission and low melting points [1,2]. Tellurium oxide (TeO_2) is a conditional glass former [2] and forms glass only with a modifier such as alkali, alkaline earth and transitional metal oxides or other glass formers. In binary tellurite glasses, the basic structural unit of TeO_4 is a trigonal bipyramid (tbp) with lone pair of electrons [3]. The application of tellurite glasses in industries such as electric, optical, electronic and other fields are immense due to their good semiconducting properties. Tellurite glasses have recently gained wide attention because of their potential as hosts of rare earth elements for the development of fibres and lasers covering all the main telecommunication bands and promising materials for optical switching devices. Recently, tellurite glasses doped with heavy metal oxides or rare earth oxides such as Gd_2O_3 , Nb_2O_5 and CeO_2 have received great scientific interest because these oxides can change the optical and physical properties of the tellurite glasses [2].

Glasses containing gadolinium ions are the subject of a great deal of interest due to their important in optical and magnetic properties for technical applications, are determined by the environment of Gd^{+3} ions, gadolinium concentration and its distribution in the glass matrix. Whereas the local structure of the Gd^{+3} sites seems to be similar in different types of glasses, the correlation

between the doping level and clustering depends on the glass type and composition [5-8].

Oxide glasses containing gadolinium ions as magnetic centers. IR analysis, Raman spectroscopy and the magnetic susceptibility measurements are carried out in this work in order to investigate the structure and magnetic properties of $0.65TeO_2$ -(0.35-x) V_2O_5 -x Gd_2O_3 glass system.

2. Experimental procedure

Glass samples with the formula $x Gd_2O_3$ -65 TeO_2 -(35-x) V_2O_5 , ($0 \leq x \leq 7.5$ mol %) were prepared by the melt-quenching technique. Required quantities of Analar grade V_2O_5 , Gd_2O_3 and TeO_2 were melted in a covered platinum crucible in an electrically heated furnace under ordinary atmospheric conditions at a temperature of about 1273 K for 2 h to homogenize the melt. The melt was stirred several times during preparation to achieve high degree of homogeneity. The melt was cast into a copper block followed by annealing at 350 °C for 2 h.

X-ray diffraction patterns were recorded to check the non-crystallinity of the glass samples using a Philips X-ray diffractometer PW/1710 with Ni-filtered, $Cu-K_{\alpha}$ radiation ($\lambda = 1.542 \text{ \AA}$) powered at 40 kV and 30 mA. The patterns (not shown) revealed broad humps characteristic of the amorphous materials and did not reveal discrete or any sharp peaks.

Infrared (IR) spectra for the glass powder (after crushing them into powder form) were obtained using an

IR Fourier spectrophotometer type JASCO, FT/IR-430 (Japan). For this purpose, each sample was mixed with KBr in the proportion of 1:100 (by weight) for 20 min and pressed into a pellet using a hand press. The spectra were recorded in the wave number range of 400-2000 cm^{-1} with a resolution of 4 cm^{-1} , corrected for dark-current noise, and normalized to eliminate the concentration effect of the powder sample in the KBr disc. The bands of the resulted spectra were fitted to enable shedding further light on the structural changes of the basic units in these glasses.

The micro-Raman spectra were taken in the backscattering configuration and analyzed using Jobin Yvon T64000 spectrometer, equipped with nitrogen cooled charge-coupled-device detector. As excitation source we used the 514.5 nm line of an Ar-ion laser.

The ac susceptibility measurements were carried out in the temperature range of 4.3–200 K at frequency 625 Hz with Lake Shore 7229 ac susceptometer using a mutual inductance bridge with an excitation field $H_{ac}=5.0$ Oe. On the basis that the magnetic susceptibility can be related to atomic properties, we converted mass magnetic susceptibility to the molar magnetic susceptibility χ_M using: $\chi_M = \chi_g \cdot M_w$, where M_w is the molecular weight of the sample.

3. Results and discussion

3.1. Structure properties

3.1.1. Infrared spectral studies

Fig. 1 shows the FTIR bands of the ternary 65 TeO_2 –(35-x) V_2O_5 -x Gd_2O_3 glasses in the range of $2.5 \leq \text{Gd}_2\text{O}_3 \leq 10$ mol %.

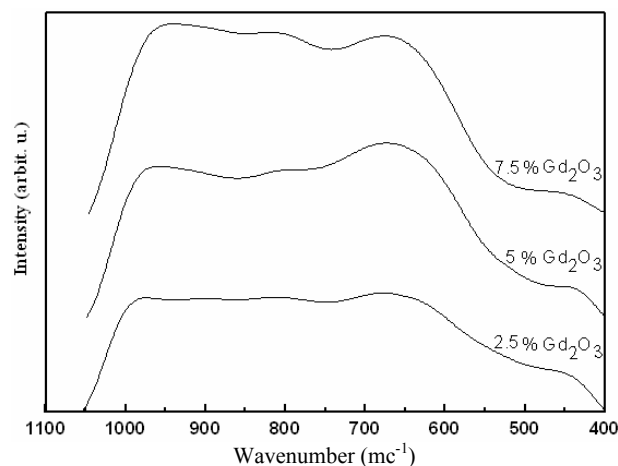


Fig. 1. IR absorption spectra of 65 TeO_2 - (35-x) V_2O_5 - x Gd_2O_3 glasses.

There are two principal broad bands in the spectra at around 675 cm^{-1} , and at 980 cm^{-1} with a shoulder at 810 cm^{-1} . The observed broadening of the bands in the spectra

of the glasses may arise for two reasons. The first is the distribution of bond angles and bond lengths and fluctuations of the local electronic and atomic environments in the amorphous state [9-12]. A second reason is the overlapping of some individual bands with each other. Each individual band has characteristic parameters such as its center (C), which is related to some type of vibrations of a specific structural group, and its relative area (A), which is proportional to the concentration of this structural group. A band fitting data process, as described elsewhere [13], should be performed to extract such parameters. The band fitting data for the investigated glasses are given in Table 1. Fig. 2 shows the band fitting of the spectra of the sample having 2.5 mol % Gd_2O_3 as an example.

Table 1. The band fitting of the Infrared spectra, where I is the intensity of the band, C is its center, and A is its relative area.

| | | | | | | | |
|-----------------------------|---|------|------|------|------|------|------|
| 2.5 Gd_2O_3 | I | 0.17 | 0.17 | 0.97 | 0.78 | 0.59 | 0.54 |
| | C | 444 | 493 | 661 | 846 | 945 | 998 |
| | A | 1.83 | 3.29 | 47.3 | 27.9 | 12.7 | 6.95 |
| 5 Gd_2O_3 | I | 0.13 | 0.11 | 0.96 | 0.71 | 0.56 | 0.44 |
| | C | 432 | 478 | 657 | 838 | 943 | 994 |
| | A | 1.22 | 1.98 | 46.7 | 30.7 | 13.3 | 6.08 |
| 7.5 Gd_2O_3 | I | 0.12 | 0.13 | 0.92 | 0.74 | 0.56 | 0.43 |
| | C | 441 | 493 | 649 | 824 | 940 | 990 |
| | A | 1.48 | 2.23 | 43.2 | 33.5 | 13.5 | 6.1 |

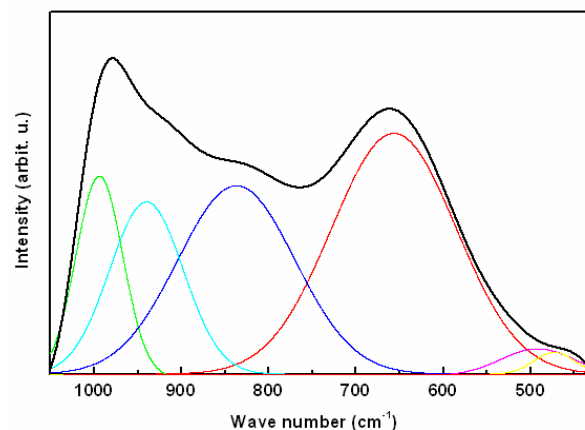


Fig. 2. The band fitting of the IR spectra of the sample having 2.5 mol % Gd_2O_3 as an example and the difference between the experimental and simulated curves.

The bands located in the range of 432-493 cm^{-1} , and 649-661 cm^{-1} are assigned to the bending mode of Te–O–Te linkages, and to the stretching mode $[\text{TeO}_4]$ trigonal pyramidal with bridging oxygen. The last band may be overlapped with a band attributed to the stretching mode of $[\text{TeO}_3]$ trigonal pyramidal with non-bridging oxygen. This mode arises from the networking of the glass

structure [14,15]. According to Table (1), it is noted that the relative area (A) of this band is constant which is referred to the constant content of TeO_2 in the glasses. The presence of the lone-pair of electrons on tellurium atoms leads to the formation of short and long equatorial $Te-O$ bonds. The higher intensity of this band refers to the smaller distortion in the TeO_4 trigonal bipyramid (tbp) units. In the case of pure V_2O_5 glass it was reported [16] that V^{5+} ions exhibit both four- and five-fold coordination states, depending on the sample preparation conditions. The IR spectrum of the amorphous V_2O_5 is characterized by the intense band in the range $1000-1020\text{ cm}^{-1}$, assigned to the vibration of isolated $V=O$ vanadyl groups in $[VO_5]$ trigonal bipyramids [17-19], the peak around $824-945\text{ cm}^{-1}$ assigned to the vibrations of $[VO_5]$ units, and the band located about $990-998\text{ cm}^{-1}$ is assigned to $[VO_4]$ units [20-23].

The examination of the FTIR spectra of the $65\text{ TeO}_2 - (35-x)\text{ V}_2\text{O}_5 - x\text{ Gd}_2\text{O}_3$ mol% shows that the increase of Gd_2O_3 content strongly modifies the characteristic IR bands as follows:

(i) The intensity of the band at around $\sim 661\text{ cm}^{-1}$ decreases and accompanied with a shift to lower wave number indicating to the appearance of TeO_4E units which corresponds to a reduction in the number TeO_3E of units with the increasing of the Gd_2O_3 content.

(ii) The peak located at about 846 cm^{-1} is shifted to lower wave number and its intensity decreases with the increasing of the Gd_2O_3 content. As was previously mentioned, the presence of this band indicates the presence of $[VO_5]$ units.

(iii) The intensity of the band from $\sim 943\text{ cm}^{-1}$ decreases with the increasing content of Gd_2O_3 and shifts to 940 cm^{-1} . This band is attributed to the $V-O$ stretching vibrations in $[VO_4]$ units.

In brief, the FTIR spectra of the studied glasses consist of four main bands and their structure is made up of $[TeO_3]$, $[TeO_4]$, tetrahedral $[VO_4]$, and $[VO_5]$ units, respectively. The presence of gadolinium cations in the glass structure lead to the appearance of a structural ordering process around the vanadium atoms as well as to a decrease in the number of linked tellurium polyhedra.

3.1.2. Raman spectral studies

The study on the structure of TeO_2 -based glasses by Raman spectroscopy has been reported by many workers [16,18,21-30]. As shown in Fig. 3, there are two pronounced peaks appeared at around 640 cm^{-1} and 815 cm^{-1} . The observed broadening of the bands in the Raman spectra needs a fitting process to extract the essential parameters C , and A .

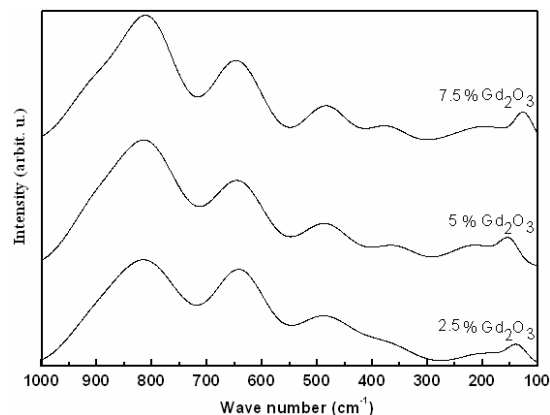


Fig. 3. Raman spectra of $65\text{ TeO}_2 - (35-x)\text{ V}_2\text{O}_5 - x\text{ Gd}_2\text{O}_3$ glasses.

The data of such a band fitting process of the investigated glasses are given in Table 2. Fig. 4 shows the band fitting of the spectra of sample having 5 mol % Gd_2O_3 as an example, and the difference between the experimental and simulated curves.

Table 2. The band fitting of the Raman spectra, where I is the intensity of the band, C is its center and A is its relative area.

| | | | | | | | | |
|------------------|---|------|------|------|------|------|------|------|
| 2.5 Gd_2O_3 | I | 0.14 | 0.12 | 0.19 | 0.46 | 0.88 | 0.99 | 0.23 |
| | C | 137 | 193 | 373 | 489 | 640 | 812 | 918 |
| | A | 1.5 | 3.61 | 5.6 | 15.5 | 26.6 | 40.9 | 6.27 |
| 5 Gd_2O_3 | I | 0.16 | 0.17 | 0.16 | 0.34 | 0.67 | 0.97 | 0.35 |
| | C | 151 | 213 | 377 | 487 | 637 | 810 | 911 |
| | A | 1.87 | 6.11 | 4.69 | 11.4 | 24 | 40.7 | 11.2 |
| 7.5 Gd_2O_3 | I | 0.19 | 0.13 | 0.13 | 0.3 | 0.65 | 0.96 | 0.42 |
| | C | 125 | 196 | 382 | 484 | 633 | 806 | 905 |
| | A | 2.37 | 5.69 | 3.73 | 9.16 | 24.5 | 38.5 | 16.1 |

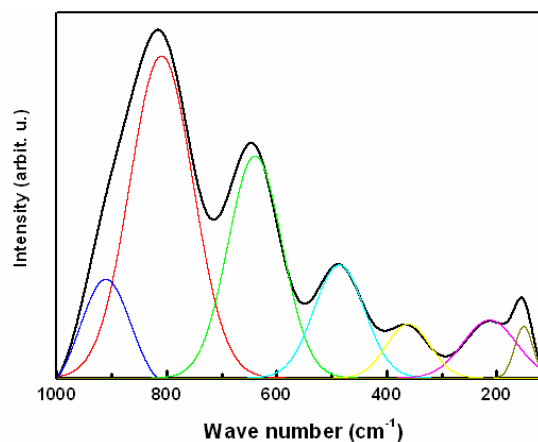


Fig. 4. The band fitting of the spectra of the sample having 5 mol % Gd_2O_3 as an example, and the difference between the experimental and simulated curves.

The peak intensity around 640 cm^{-1} , which is assigned to a stretching vibration of TeO_4 tbp (trigonal bipyramids) units was observed to increase as the Gd_2O_3 contents increases. The decrease in intensity suggests the possibility of conversion from TeO_3 tbp units to the other basic structural unit (TeO_4) [27]. Other peaks around 487 cm^{-1} , are observed to be less sensitive to the Gd_2O_3 contents. A decrease in the peak intensity would suggest the occurrence of the destruction of Te–O–Te (or O–Te–O) linkages [31], thus resulted in the decreasing of the Te–O–Te linkages in a continue network of TeO_n ($n = 4, 3 + 1$, and/or 3) entities, which is consistent with the observation reported elsewhere [18]. Another peaks that might be of interest occur around $200\text{--}370\text{ cm}^{-1}$ which can be assigned to both TeO_3 tp and Gd–O bond [29]. As this peaks become decreasingly sharper it can be said that the TeO_3 tp structural unit decreases as the Gd_2O_3 content increases. This argument is in agreement to an earlier work [29]. Thus it can be said that Gd^{3+} in the glass may significantly modified the Te–O networking structure.

On the other hand, there is a band at $\sim 810\text{ cm}^{-1}$, is attributed to O–V–O stretching vibration [32,35] and a band at $\sim 910\text{ cm}^{-1}$ is attributed to V=O vibration in the tetragonal pyramid of V_2O_5 [33]. Furthermore the increasing intensity of the band at $\sim 910\text{ cm}^{-1}$ assigned to O–V–O and V–O–V groups underline the breaking of the tellurite chains and V_2O_5 tend to act as a network former [34]. Furthermore the increasing intensity of the band at $\sim 910\text{ cm}^{-1}$ assigned to O–V–O and V–O–V groups underline the breaking of the tellurite chains and V_2O_5 tendency to act as a network former.

3.2. Magnetic properties

Temperature dependence of the susceptibility χ of paramagnetic materials shows a Curie–Weiss type behavior which can be expressed as follows [36,37]:

$$\chi_M = \chi_{diam.} + \frac{C_M}{T - \theta_p}, \quad (1a)$$

where

$$C_M = \frac{\mu_{eff.}^2 \cdot N_A}{3k_B} x, \quad (1b)$$

$\chi_{diam.}$ is the susceptibility of the host lattice, C_M is molar Curie constant, θ_p is the paramagnetic Curie temperature, T is absolute temperature in kelvins, N_A is the Avogadro number, x is the mole part of Gd^{3+} ions in the glass, k_B the Boltzmann constant, $\mu_{eff.}$ is the effective magnetic moment. The ac magnetic susceptibility results for these glasses are displayed in Fig. 5 as a plots of the magnetic susceptibility as a function of the temperature T . The data appear to follow a Curie–Weiss type behavior over the most of temperature range. All the

measured curves are fitted according to the modified Curie–Weiss law in the temperature range 20–200 K, because it is a more straight line in these range. Values of the paramagnetic Curie temperature θ_p were determined for each of the glassy samples and tabulated in Table 3. The magnitude of the paramagnetic Curie temperature θ_p increases with increasing the Gd content in the glass. Since the paramagnetic Curie temperature θ_p , is a rough measure of the strength of the interaction between the magnetic ions in the sample. the higher value implies stronger interaction and/or more ions participating in the interaction. The negative values for the paramagnetic Curie temperatures indicate that the magnetic interaction is predominately antiferromagnetic in these gadolinium vanado-tellurite glasses [36].

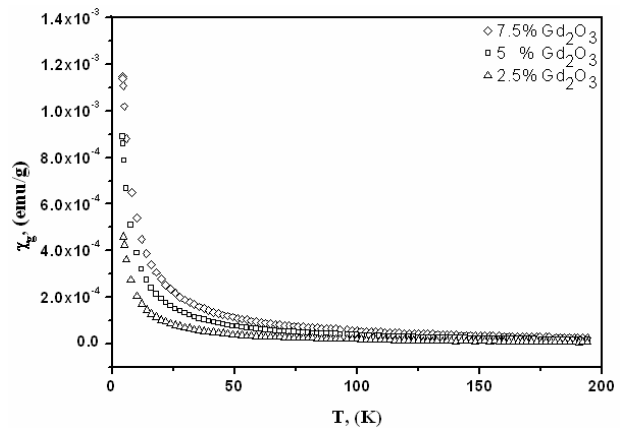


Fig. 5. Ac magnetic susceptibility versus temperature for $65\text{TeO}_2 - (35-x)\text{V}_2\text{O}_5 - x\text{Gd}_2\text{O}_3$ glasses ($x=2.5, 5, 7.5$).

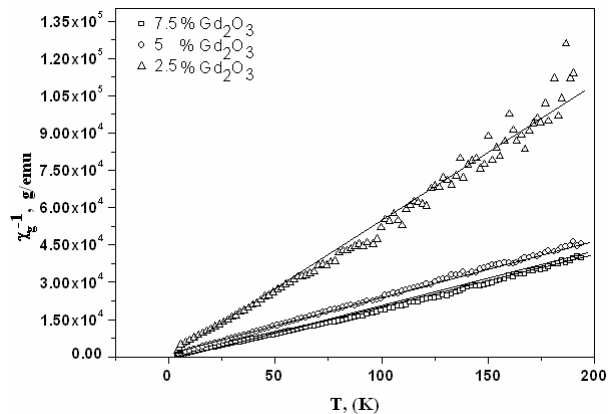


Fig. 6. The inverse of the magnetic susceptibility as a function of the temperature for $65\text{TeO}_2 - (35-x)\text{V}_2\text{O}_5 - x\text{Gd}_2\text{O}_3$ glasses.

The experimental effective magnetic moment of the gadolinium ions calculated from the experimentally determined C_M values as:

$$\mu_{\text{eff.}} = 2.827 \sqrt{\frac{C_M}{2x}}, \quad (2)$$

The calculated values of the magnetic moment are given in Table. 3 which in a good agreement with the reported value of the atomic magnetic moment of Gd⁺³ ions in free ion state: $\mu_{\text{Gd}^{+3}} = 7.98 \mu_B$. The small negative values of θ_p , $\theta_p < -2$ K suggest the presence of weak antiferromagnetic interaction. The assumption of the antiferromagnetic nature of the interaction between the Gd⁺³ ions is also supported by the fact that the effective magnetic moment per gadolinium ion, is less than the magnetic moment of the free gadolinium ion $\mu_{\text{Gd}^{+3}}$.

Using the molecular field model [38], the molecular field constant J is given by:

$$J = \frac{\theta_p}{C_M} = \frac{2zJ_{ij}}{N \cdot g^2 \cdot \mu_B^2}, \quad (3)$$

where N and Z are the total and exchange-coupled number of magnetic ions, J_{ij} is the magnetic exchange integral, g is their spectroscopic splitting factor and μ_B is the Bohr magneton. The calculated values of $J = \theta_p / C_M$ from the experimental data are given in Table 3.

Table 3. Magnetic parameters of TeO₂-V₂O₅-Gd₂O₃ glassy system.

| % Gd ₂ O ₃ | θ_p , K | $\mu_{\text{eff.}}$, μ_B | J |
|----------------------------------|-------------------|----------------------------------|-------|
| 2.5 | -0.440 | 7.602 | 0.012 |
| 5 | -0.446 | 7.196 | 0.011 |
| 7.5 | -1.697 | 6.601 | 0.021 |

It is clear that the molecular field theory is approximately increased with increasing the gadolinium ions content. Supposed, in a first approximation, that z increases when N increases, so allowed that z/N is constant (the number of gadolinium ions that interact is proportional with the total number of gadolinium ions), results that the molecular field constant is proportional with the magnetic exchange integral. So that, the values of the magnetic exchange integral increase when the content of gadolinium ions increase in studied glasses. The ac magnetic susceptibility data obtained for TeO₂-V₂O₅-Gd₂O₃ glasses are in agreement with those previously reported for other oxide glasses containing gadolinium ions [39-42,5].

4. Conclusions

The analysis by IR and Raman spectroscopy indicates the presence of four main bands and their structure is made up of [TeO₃], [TeO₄], tetrahedral [VO₄], and [VO₅] units, respectively. The presence of gadolinium cations in the glass structure lead to the appearance of a structural ordering process around the vanadium atoms as well as to a decrease in the number of linked tellurium polyhedra. Thus, it can be said that Gd⁺³ in the glass may significantly modify the Te-O networking structure. The samples are paramagnetic following the Curie-Weiss law in a wide range of temperatures. Values of θ_p suggest predominately the presence of weak antiferromagnetic interaction in these gadolinium vanado-tellurite glasses

Acknowledgments

One of the authors (I.S. Yahia) would like to acknowledge the financial support from partnership and ownership initiative (PAROWN) of Egyptian Ministry of Higher Education and State for Scientific research.

References

- [1] Y. Saddeek, Mater. Chem. Phys., **91**, 146 (2005).
- [2] B. Eraiah, Bull. Mater. Sci. **29**, 375 (2006).
- [3] E. F. Lambson, G. A. Saunders, B. Bridge, R. A. Mallawany, J. Non-Cryst. Solids **69**, 117 (1984).
- [4] V. Rajendran, N. Palanivelu, B. K. Chaudhuri, K. Goswami, J. Non-Cryst. Solids **320**, 195 (2003).
- [5] I. Ardelean, L. Griguta, J. Non-Cryst. Solids **353**, 2363 (2007).
- [6] I. V. Chepeleva, V. N. Lazukin, Dokl. Akad. Nauk SSSR **226**, 311 (1976).
- [7] C. M. Brodbeck, L. E. Iton, J. Chem. Phys. **83**, 4285 (1985).
- [8] L. Cugunov, A. Mednis, J. Kliava, J. Phys.: Condens. Matter **3**, 8017 (1991).
- [9] I. Shaltout, Y. Tang, R. Braunstein, E. Shaisha, J. Phys. Chem. Solids **57**, 1223 (1996).
- [10] P. Charton, L. Gengembre, P. Armand, J. Sol. Stat. Chem. **168**, 175 (2002).
- [11] Y. Dimitriev, V. Dimitrov, M. Arnaudov, J. Mater. Sci. **18**, 1353 (1983).
- [12] M. Arnaudov, V. Dimitrov, Y. Dimitriev, L. Markova, Mater. Res. Bull. **17**, 1121 (1982).
- [13] B. Stuart, Infrared Spectroscopy: Fundamentals and Applications, John Wiley & Sons Ltd., 2004.
- [14] T. Sekiya, N. Mochida, S. Ogawa, J. Non-Cryst Solids **176**, 105 (1994).
- [15] I. Shaltout, Y. Tang, R. Braunstein, A. M. Abu-Elazm, J. Phys. Chem. Solids **56**, 141 (1995).
- [16] J. Mendialdua, R. Casanova, Y. Barbaux, J. Electron Spectrosc. Relat. Phenom. **71**, 249 (1995).
- [17] H. Miyata, K. Fujii, T. Ono, Y. Kubokawa, T. Ohno, F. Hatayama, J. Chem. Soc. Faraday Trans. **83**, 675 (1987).

- [18] E. Culea, Al. Nicula, I. Bratu, *Phys. Stat. Sol.* **83**, K15 (1984).
- [19] V. Dimitrov, *J. Solid State Chem.* **66**, 256 (1987).
- [20] G. D. Khattak, N. Tabet, L. E. Wenger, *Phys. Rev. B*, **72**, 104202 (2005).
- [21] D. de Waal, C. Hutter, *Mater. Res. Bull.* **29**, 843 (1994).
- [22] D. Manara, A. Grandjean, O. Pinet, J. L. Dussossoy, D. R. Neuville, *J. Non-Cryst. Solid* **353**, 12 (2007).
- [23] S. Rada, E. Culea, V. Rus, M. Pica, M. Culea, *J. Mater. Sci.* **43**, 3713 (2008).
- [24] P. Charton, P. Thomas, P. Armand, *J. Non-Cryst. Solids* **321**, 81 (2003).
- [25] V. Nazabal, S. Todoroki, A. Nukui, T. Matsumoto, S. Suehara, T. Hondo, T. Araki, S. Inoue, C. Rivero, T. Cardinal, *J. Non-Cryst. Solids* **325**, 85 (2003).
- [26] S. Kawasaki, T. Honma, Y. Benino, T. Pujiwara, R. Sato, T. Komatsu, *J. Non-Cryst. Solids* **325**, 61 (2003).
- [27] H. Li, Y. Su, S. K. Sundaram, *J. Non-Cryst. Solids* **293–295**, 402 (2001).
- [28] J. C. Sabadel Armand, D. Cachau-Herreillat, P. Baldeck, O. Doclot, A. Ibanez, E. Philippot, *J. Solid State Chem.* **132**, 411 (1997).
- [29] T. Komatsu, H. Tawarayama, H. Mohri, K. Matusita, *J. Non-Cryst. Solids* **135**, 105 (1991).
- [30] L. Hu, Z. Jiang, *Phys. Chem. Glasses* **37**(1), 19 (1996).
- [31] L. Laversenne, Y. Guyot, C. Goutaudier, M. Th. Cohen-Adad, G. Boulon, *Optical Materials* **16**, 475 (2001).
- [32] J. E. Pemberton, L. Latifzadeh, J. Fletcher, S. H. Risbud, *Chem. Mater.* **3**, 195 (1991).
- [33] J. Garbarczyk, P. Machowski, M. Wasincionek, L. Tykars, R. Bacewicz, A. Aleksiejuk, *Solid State Ionics* **136–137**, 1077 (2000).
- [34] G. Le Saout, P. Simon, F. Fayon, A. Blin, Y. Vaills, *J. Raman Spectrosc.* **33**, 740 (2002).
- [35] N. Vedeanu, O. Cozar, I. Ardelean, B. Lendl, D. A. Magdas, *Vibrational Spectroscopy* **48**, 259 (2008).
- [36] M. A. Salim, G. D. Khattak, P. S. Fodor, L. E. Wenger, *J. of Non-Crystalline Solids* **289**, 185 (2001).
- [37] A. Fern´andez, X. Bohigas, J. Tejada, E. A. Sulyanova, I. I. Buchinskaya, B. P. Sobolev, *Materials Chemistry and Physics* **105**, 62 (2007).
- [38] L. F. Bates, *Modern Magnetism*, Cambridge University, London, 133, 1962.
- [39] I. Ardelean, E. Burzo, D. Mitulescu-Ungur, S. Simon, *J. Non-Cryst. Solids* **146**, 256 (1992).
- [40] E. Culea, I. Milea, *J. Non-Cryst. Solids* **189**, 246 (1995).
- [41] S. Simon, I. Ardelean, S. Filip, I. Bratu, I. Cosma, *Solid State Commun.* **116**, 83 (2000).
- [42] E. Culea, L. Pop, S. Simon, *Mater. Sci. Eng. B* **112**, 59 (2004).

*Corresponding author: dr_isyahia@yahoo.com
isyahia@gmail.com